Seasonal and diel variation in greenhouse gas emissions from an urban pond and its major drivers

Tamara J. H. M. van Bergen [ID],[1,2]* **Nathan Barros,**[1,3] **Raquel Mendonça,**[1,3] **Ralf C. H. Aben,**[1]
Inge H. J. Althuizen,[1,4] **Vera Huszar,**[5] **Leon P. M. Lamers,**[1] **Miquel Lürling,**[6] **Fábio Roland,**[3]
Sarian Kosten [ID][1]

[1]Department of Aquatic Ecology and Environmental Biology, Institute for Water and Wetland Research, Radboud University, Nijmegen, The Netherlands
[2]Department of Environmental Science, Institute for Water and Wetland Research, Radboud University, Nijmegen, The Netherlands
[3]Laboratory of Aquatic Ecology, Institute of Biology, Federal University of Juiz de Fora, Juiz de Fora, Brazil
[4]Department of Biological Sciences and Bjerknes Centre for Climate Research, University of Bergen, Bergen, Norway
[5]Department of Botany, National Museum, Federal University of Rio de Janeiro, Rio de Janeiro, Brazil
[6]Aquatic Ecology and Water Quality Management Group, Wageningen University, Wageningen, The Netherlands

Abstract

Small water systems are important hotspots of greenhouse gas (GHG) emission, but estimates are poorly constrained as data are scarce. Small ponds are often constructed in urban areas, where they receive large amounts of nutrients and therefore tend to be highly productive. Here, we investigated GHG emissions, seasonal and diel variation, and net ecosystem production (NEP) from an urban pond. In monthly 24-h field campaigns during 11 months, diffusive water–atmosphere methane (CH_4) and carbon dioxide (CO_2) fluxes and CH_4 ebullition and oxidation were quantified. With oxygen (O_2) measurements, NEP was assessed. The pond was a net GHG source the entire year, with an emission of 3.4 kg CO_2 eq m^{-2} yr^{-1}. The dominant GHG emission pathway was CH_4 ebullition (bubble flux, 50%), followed by diffusive emissions of CO_2 (38%) and CH_4 (12%). Sediment CH_4 release was primarily driven by temperature and especially ebullition increased exponentially above a temperature threshold of 15°C. The pond's atmospheric CO_2 exchange was not related to NEP or temperature but likely to a high allochthonous carbon (C) input via runoff and anaerobic mineralization of C. We expect urban ponds to show a large increase in GHG emission with increasing temperature, which should be considered carefully when constructing ponds in urban areas. Emissions may partly be counteracted by pond management focusing on a reduction of nutrient and organic matter input.

Although lakes and ponds only cover a small area of the Earth's nonglaciated land area (~ 4%; Verpoorter et al. 2014), they play a disproportionally large role in the global carbon cycle due to the large amount of C they process, store, and transport (Tranvik et al. 2009). The majority of lakes and ponds is a significant source of CO_2 and CH_4 to the atmosphere (Cole et al. 1994; Bastviken et al. 2011), while at the same time, they bury large amounts of C in their sediments (Dean and Gorham 1998; Mendonça et al. 2017). Carbon

emission in lakes and ponds is largely driven by hydrological CO_2 inputs (Weyhenmeyer et al. 2015; Wilkinson et al. 2016) and by mineralization of organic matter (OM) within the system (Algesten et al. 2003). Conversely, primary producers can assimilate CO_2 at such high rates that the system turns into a CO_2 sink (Roland et al. 2010; Pacheco et al. 2013). However, global and regional studies suggest that only a small portion of lakes (6–14%) is undersaturated with respect to the atmospheric CO_2 (Cole et al. 1994; Kosten et al. 2010).

Annually, lentic inland waters emit 0.3 Pg C as CO_2 (Raymond et al. 2013) and 0.08 Pg C as CH_4 (Bastviken et al. 2011). This last value may be an underestimate, as ebullition is likely underestimated (Wik et al. 2016). Although small waterbodies (< 50 ha) comprise 98% of lentic inland waters by number and one third by volume (Downing et al. 2006; Verpoorter et al. 2014), small lakes and ponds are strongly underrepresented in literature (Downing 2010), and greenhouse gas

Additional Supporting Information may be found in the online version of this article.

(GHG) inventories such as the United Nations Framework Convention on Climate Change. Yet, these small systems are estimated to be responsible for 15% and 41% of the global CO_2 and CH_4 diffusive emission from lentic freshwaters, respectively, and thus are important hotspots of C emission (Holgerson and Raymond 2016).

Here, we investigated GHG emissions from a small nutrient-rich urban pond. Ponds in urban areas are constructed for recreational reasons and also for microclimate regulation, for rainwater storage, or as ornamental features to improve public open spaces (Bolund and Hunhammar 1999). They provide several ecosystem services that enhance human wellbeing (e.g., recreation and microclimate regulation), but ponds also enhance biodiversity by increasing ecological connectivity in urban areas (Gledhill et al. 2008). Since the end of the 19th century, urbanization has increased exponentially and is expected to keep increasing, especially in developing countries (Champion 2001). Urban ponds are mostly shallow and stagnant, which makes them highly susceptible to anthropogenic disturbances and eutrophication (Waajen et al. 2014). They generally receive a large amount of nutrients, for example, from bird droppings, sewage overflow, and stormwater runoff (Scherer et al. 1995; Novotny 1999; Waschbusch et al. 1999; Wong et al. 2000), which frequently leads to phytoplankton blooms (Waajen et al. 2014) and could affect GHG emission.

Especially the high perimeter to surface area ratio of small urban ponds could result in a relatively high input of terrestrial OM, which may play an important role in fueling heterotrophic respiration (Hanson et al. 2007). Even though eutrophic systems tend to have a high gross primary production (GPP; Smith 1979; Balmer and Downing 2011), ecosystem respiration (ER) tends to be high in these systems as well (Sand-Jensen and Staehr 2009). Hence, while in some eutrophic systems, the high primary production rates may lead to a net uptake of CO_2 (Pacheco et al. 2013), this is not necessarily the case as ER and the inflow of CO_2 via surface or groundwater may outweigh the primary producers' CO_2 uptake (Casper et al. 2000; Trolle et al. 2012). In addition, the high OM input, together with the phytoplankton-derived C that tends to be easily degradable, potentially leads to high CH_4 production rates in urban ponds (West et al. 2012; West et al. 2016; Martinez-Cruz et al. 2017).

The high relative contribution of small ponds to freshwater GHG emissions in combination with the scarcity of data regarding pond GHG emissions was our rationale for quantifying whole-year water–atmosphere CO_2 and CH_4 fluxes and their seasonal and diel variation in an urban pond. With an intensive measurement campaign, we aimed to not only quantify CO_2 and CH_4 emission from a temperate and hypereutrophic urban pond but also to obtain insight in temporal and spatial variation of fluxes to optimize future efforts to quantify GHG emissions from small systems. Additionally, we aimed to identify the main ecosystem components—sediment, phytoplankton, heterotrophic picoplankton, and fish—responsible for the within-system CO_2 production and consumption. Our approach combined daytime

and nighttime field measurements on a monthly basis with laboratory assays and modeling.

We hypothesized the pond to be an important GHG emitter as well as an important C sink, with a higher CH_4 emission during warm months. We further hypothesized that the pond would shift between a net C source in fall and winter to a net C sink in spring and summer, mainly due to fluctuations in CO_2 emission caused by phytoplankton growth—i.e., high CO_2 uptake by photosynthesis in summer and much less so in winter. Because of the high primary production, we also expected a high variability in diel CO_2 emission, especially in summer. Due to the shallowness of the pond (average depth of 1.3 m), we expected the sediment to be a major contributor to CO_2 emission but simultaneously an important site for C burial because of a high OM loading.

Materials and methods

In the field, we measured diffusive water–atmosphere fluxes of CH_4 and CO_2, ebullitive CH_4 fluxes, water layer CH_4 oxidation rates, and diel oxygen (O_2) concentrations. The pond's net ecosystem production (NEP), GPP, and ER were calculated from O_2 concentrations. A metabolic model was constructed that included aerobic respiration estimates for each organism group (organisms in the sediment, phytoplankton, heterotrophic picoplankton, and fish), based on temperature and O_2 consumption. The outcome of both the field and laboratory measurements, combined with data from an existing hydrological model for the pond area, and literature data, were joined in a mass balance to unravel the major contributors to the CO_2 flux. Finally, C burial rates in the pond were determined in order to compare C burial and emission rates.

Study site and sampling strategy

This study was performed in manmade urban pond situated in Malden, Gelderland, the Netherlands ("Korte Loef," 51°46′30″N, 5°51′11.22″E). The pond was constructed in 1994 to function as a rainwater overflow for the surrounding urban area. It covers an area of 4635 m^2, stores approximately 6000 m^3 of water, and has distinct central (± 2 m) and littoral (≤ 1 m) zones (respectively, 44% and 56% of the total surface area). Monthly field campaigns were performed from July 2013 till May 2014. During the field campaigns, measurements were performed over 24-h periods at two sampling stations, one in the central and one in the littoral zone, that were placed at the same location every field campaign. Groundwater samples were taken from a well situated 20 m from the shore. Every 15 min, the O_2 concentration, temperature, and pH were measured. Diffusive gas fluxes were measured every 3 h during the campaign, whereas methane ebullition and oxidation were measured separately in the light and dark period. We did not sample in June due to logistic reasons, therefore values for this month were interpolated using the average values of May and July in order to obtain year-round estimates. Areal estimates of gas fluxes for the entire pond were calculated based on the

weighted average of the central and littoral area. In our analyses, we considered the months June, July, and August as the summer season; September, October, and November as fall; December, January, and February as winter; and March, April, and May as spring.

Water chemistry

A depth integrated water sample was taken from each of the sampling stations once per field campaign for chemical analyses. Unfiltered water samples were analyzed for total phosphorus (TP), by inductively coupled plasma spectrometry (ICP-OES iCAP 6000, Thermo Fisher Scientific), and for total inorganic nitrogen (TIN) by measuring and summing the ammonium (NH_4^+) and nitrate (NO_3^-) concentrations. Ammonium and nitrate were measured colorimetrically with an Auto Analyzer 3 system (Bran & Luebbe), using salicylate (Grasshoff and Johannsen 1972) and hydrazine sulfate (Kamphake et al. 1967), respectively. Phytoplankton chlorophyll-α (Chl α) concentration and division over major groups (brown, green, and blue Chl α) were determined using a phytoplankton analyzer system with a portable emitter–detector unit (Phyto-PAM and Phyto-ED, Walz).

O_2, temperature, and pH

During the monthly 24-h field campaigns, we deployed a multiparameter portable meter (HQ40d, Hach) equipped with a luminescent/optical dissolved oxygen probe (LDO101) fitted with a temperature and barometric pressure sensor (model LDO101) and a pH–temperature sensor (model 9156BNWP) at the littoral and at the central station, at 0.5 m depth. Dissolved O_2 concentration, temperature, pH, and barometric pressure were recorded every 15 min. A third multimeter was used to sample vertical dissolved O_2 and temperature profiles at both stations every 3 h.

CO_2 and CH_4 emission

Diffusive CO_2 and CH_4 fluxes across the air–water interface were measured using a transparent Plexiglas floating chamber (30 cm diameter, 20 cm height) connected to a GHG analyzer (GGA) using Off-axis ICOS technology (GGA-24r-EP, Los Gatos Research). A closed loop between the chamber and the detector was established using an inlet and outlet on the top of the chamber. A third opening, fitted with an air-tight screw cap, was used to equilibrate the chamber with atmospheric pressure prior to each measurement. Measurements were conducted every 3 h, by placing the chamber three times (treated as triplicates) at the central and littoral zone. Each measurement took about 200 s, and the GGA was configured to log data every second. The flux of CO_2 and CH_4 was calculated based on the slope of the relationship between the concentration in the chamber headspace and time:

$$F = (V/A) \times \text{slope} \times [(P \times F1 \times F2)/(R \times T)] \tag{1}$$

where F is the gas flux (g m^{-2} d^{-1}), V is the chamber volume (m^3), A is the chamber surface area (m^2), slope is the slope of the relationship between the CH_4 or CO_2 concentration and the time (ppm s^{-1}), P is atmospheric pressure (Pa), $F1$ is molar mass of CO_2 (44) or CH_4 (16) (g mole^{-1}), $F2$ is the conversion factor of seconds to days, R is gas constant 8.3145 (m^3 Pa K^{-1} mol^{-1}), and T is temperature (K). The values from the triplicate measurements were averaged to give the flux of each station (i.e., central or littoral zone). The fluxes of CO_2 and CH_4 were multiplied by their global warming potential (GWP, 1 and 34 over a 100 yr time horizon, respectively; Myhre et al. 2013) and then summed to obtain the total GHG flux in CO_2 equivalents (CO_2 eq).

Ebullition

In order to quantify the spontaneous release of bubbles from sediments to the atmosphere (ebullition), three inverted funnels with a diameter of 35 cm were connected to water-filled infusion bottles (volume of 0.5 liter) and employed at the pelagic zone of the pond (as in Almeida et al. [2016]). Infusion bottles were replaced at sunset or sundown, and after collection, the gas volume was measured by subtracting the weight of each bottle from the full filled weight (i.e., completely filled with water) of the bottle. The CH_4 concentration of the gas was analyzed on a HP 5890 gas chromatograph equipped with a Porapak Q column (80/100 mesh) and a flame ionization detector (GC-FID, Hewlett Packard).

CH_4 oxidation and sediment CH_4 release

CH_4 oxidation was measured as the decline in CH_4 concentration over time (as in Bastviken et al. [2008]), in three flexible medical blood bags (volume 500 mL) located in the shallow (0.5 m) or deep (1 or 2 m, depending on whether it was the littoral or central zone, respectively) part of the water column, in each sampling station. Separate blood bags were incubated with pond water from the corresponding depth, during day and night to evaluate potential temporal differences in CH_4 oxidation. The exact same procedure was followed as in Almeida et al. (2016). As a proxy for sediment CH_4 release, we used the sum of quantified CH_4 oxidation, CH_4 water–atmosphere diffusion, and CH_4 ebullition. In months where no CH_4 oxidation was quantified due to technical difficulties (January and May), oxidation was estimated as a function of the diffusive CH_4 flux. The rationale behind this is that the methane oxidation rate strongly dependents on the methane concentration, which, in turn, affects CH_4 diffusion (CH_4 oxidation $= 0.0476 \times$ exp $[28.97 \times CH_4$ diffusion]; $R^2_{adj} = 0.87$).

NEP and respiration by different organism groups

We used 15-min interval O_2 measurements to calculate the O_2 change over time (ΔO_2; g O_2 L^{-1} h^{-1}) and subsequently calculated NEP by integrating ΔO_2 over 24 h (as in Cole et al. [2000] and Staehr et al. [2010]). From the NEP, GPP, and ER were calculated (*see* Supporting Information SI 1 for details). Subsequently, we distinguished different organism groups

contributing to the aerobic ER in the pond: phytoplankton, heterotrophic picoplankton, and methanotrophs in the water layer; organisms in the sediment; and fish. To assess the contribution of all separate organism groups to the ER, we constructed a metabolic model consisting of the relationship between water temperature and O_2 consumption for each organism group. These relationships were based on incubations and—for fish respiration—on literature-derived relationships (*see* Supporting Information SI 2 for details).

Hydrological inputs and within-pond CO_2 production

For each season, we assessed the relative importance of hydrological CO_2 input via groundwater, within-pond CO_2 production from ecosystem productivity (NEP) and from photochemical mineralization of chromophoric dissolved organic carbon (cDOC) (see Supporting Information SI 3 for details). The CO_2 input from groundwater was calculated based on the estimated groundwater inflow and the CO_2 concentration in the groundwater. Photochemical mineralization cDOC was calculated as a direct response to solar radiation exposure and solely based on the average daily light intensity (as in Vähätalo et al. [2000] and Weyhenmeyer et al. [2015]). Light intensity data were obtained from weather station Volkel, Noord-Brabant, The Netherlands.

C burial

Organic C burial rates were estimated by taking six sediment cores (6 cm diameter) with a piston sampler at locations distributed over the central zone of the pond, determining total C content and dividing the estimated areal C stock of the pond by its age (according to Mendonça et al. [2014]; *see* Supporting Information SI 4 for details).

Statistics

All statistical analyses were performed using R (version 3.5.0). Statistical significance was determined at $p < 0.05$. The effect of location (littoral or center) and time of day (day or night) on GHG fluxes and methane oxidation were tested using linear mixed-effects and generalized linear mixed-effects models (LMM and GLMM, respectively) using the "lme4" package (Bates et al. 2015; *see* Supporting Information SI 5 for details). For methane oxidation, the effect of water depth (shallow or deep) was also evaluated. Assumptions of linearity, homoscedasticity, and normality were checked by visual inspection of residual plots and a Shapiro Wilk's test (function *shapiro.test*), respectively (*see* Supporting Information SI 5 for details). Simple linear regression and nonlinear regression were performed using the *lm* and *nls* function, respectively. Coefficients and p values for Pearson correlations were obtained using the rcorr function ("Hmisc" package). All error values in the manuscript give the standard deviation.

Results

Water chemistry

The yearly average concentrations of TP and TIN were 4.5 ± 0.9 and 54.0 ± 32.3 μmol L^{-1}, respectively. The average

Chl α concentration was 81 ± 29 μg L^{-1}, with the lowest concentration observed in April (37 μg L^{-1}) and highest concentration in July (119 μg L^{-1}). The water layer was dominated by cyanobacteria during summer and fall and by green algae during winter and spring. The observed water temperature varied from $4.3°$C during winter to $27.8°$C during summer and was $13.0°$C $\pm 0.7°$C on average. The O_2 concentration, measured at 0.5 m depth, varied between 1.6 and 13.5 mg L^{-1} during the year and was on average 9.1 ± 2.6 mg L^{-1}. The O_2 concentration near the bottom of the pond ranged between approximately 0 and 11 mg L^{-1}. During July, August, and September, diurnal stratification occurred, with mixing occurring at night. During the other months, the pond was homogeneously mixed all day. The pH had a neutral value on average (7.2 ± 0.2), with slightly acidic values in summer (pH around 6.5) and slightly basic values in spring and fall (pH around 8).

Carbon flux and burial

The urban pond was a net C source all year with an average C (CO_2-C and CH_4-C) emission of 1.07 ± 0.43 g C m^{-2} d^{-1}. On average, the diffusive CO_2 emission was 0.95 ± 0.40 g CO_2-C m^{-2} d^{-1}, with the highest values measured in summer and winter season (Figs. 1, 3). CO_2 diffusion was not related to temperature ($F_{1,9} = 0.204$; $p = 0.66$, $R^2 = 0.02$) or Chl α concentration ($F_{1,9} = 0.008$; $p = 0.93$, $R^2 = 0.001$). Both diffusive and ebullitive CH_4 emission were positively related to temperature ($R^2_{adj} = 0.86$ and $R^2_{adj} = 0.82$, respectively), and thus similarly the total CH_4 emission as a sum of these fluxes was positively related to temperature (Fig. 2). The diffusive and ebullitive CH_4 emission were, respectively, 0.02 ± 0.30 and 0.10 ± 0.49 g CH_4-C m^{-2} d^{-1}. Most CH_4 was emitted via the ebullitive emission pathway (75%), and only approximately 25% was emitted via diffusion. When taking the GWP into account, we found a yearly GHG emission (CO_2 and CH_4 emission combined) of 9.19 ± 7.99 g CO_2 eq m^{-2} d^{-1}. The yearly average ebullitive CH_4 emission was 4.63 ± 6.70 g CO_2 eq m^{-2} d^{-1}, which was considerably higher than the other fluxes. The yearly average diffusive CO_2 and CH_4 emissions were respectively 3.46 ± 1.48 and 1.09 ± 4.09 g CO_2 eq m^{-2} d^{-1}. An annual average C burial rate of 29 g C m^{-2} yr^{-1} was found, which is substantially lower than the annual C emission (CO_2 and CH_4 emission combined) of 391 g C m^{-2} yr^{-1}.

Sediment CH_4 release and CH_4 oxidation

The sediment CH_4 release was estimated by summing the average CH_4 diffusion, ebullition, and oxidation in the water column for each month. The estimated sediment CH_4 release was positively related to water temperature (T_w), with the highest release rate observed at the highest water temperature (Fig. 2). There seems to be a threshold around $15°$C, above which the sediment CH_4 release increases substantially (from April up to and including September). The estimated sediment CH_4 release varied considerably throughout the year, from 0.01 ± 0.005 g CH_4-C m^{-2} d^{-1} in March to 1.04 ± 0.46 g CH_4-C m^{-2} d^{-1} in July (Fig. 2). The percentage of estimated sediment CH_4 emission that was oxidized

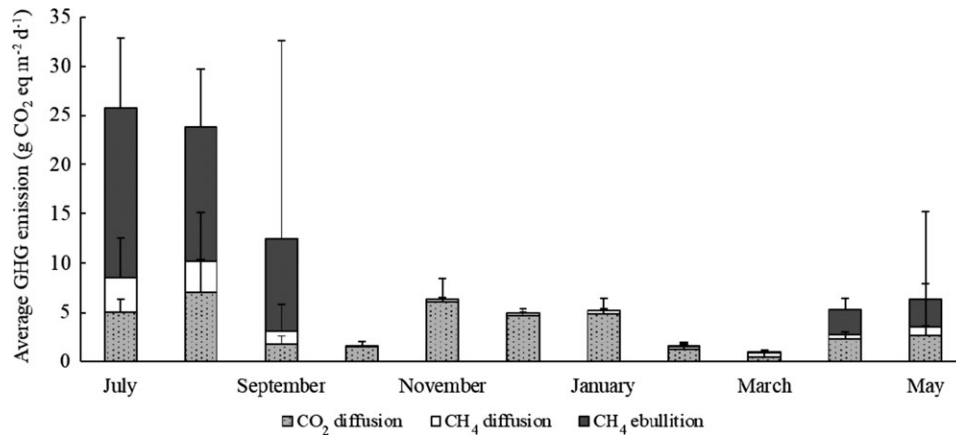**Fig. 1.** Measured CO_2 diffusion, CH_4 diffusion, and CH_4 ebullition in CO_2 equivalents (g CO_2 eq m^{-2} d^{-1}) $\pm$ SD. At some dates, the error bars (SD) are too small to show in the figure.
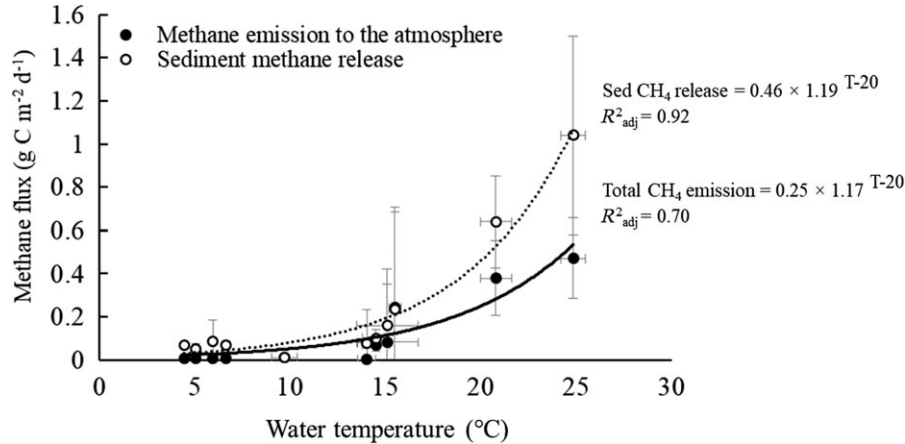

Fig. 2. Relationship between water temperature and CH_4 fluxes in the pond. All average values are shown with their standard deviation, but at some dates, the error bars are too small to show. The solid line shows the relationship of water temperature with the average total CH_4 emission to the atmosphere (black dots), which includes water–atmosphere diffusion and ebullition. The dashed line shows the relationship of water temperature with sediment CH_4 release (white dots), which was calculated as the sum of water–atmosphere CH_4 diffusion and ebullition and water column CH_4 oxidation. Note that CH_4 oxidation rates were not measured in January and May. In these months, we estimated CH_4 oxidation rates based on the relationship between CH_4 diffusion and oxidation (*see* Materials and Methods section).

before reaching the atmosphere, varied from 0% to 97% over the year (average 57%), with values ranging between 0 and 0.58 g CH_4-C m^{-2} d^{-1}. On average, 0.16 g CH_4-C m^{-2} d^{-1} was oxidized. We found a significant location–depth interaction effect (GLMM: Wald $Z = 6.31$; $p < 0.001$): the effect of deep vs. shallow incubation on CH_4 oxidation rates is larger for the littoral than the central zone of the pond. There was also a significant time–location–depth interaction (GLMM: Wald $Z = -15.59$; $p < 0.001$).

Temporal and spatial variation in C fluxes

The $CO_2 : CH_4$ emission ratio (in CO_2 equivalents) varied strongly over the year (Supporting Information Table S2). In March, the ratio was 1 and there was an equal share of GHG emitted. From April until September, the ratio was well below 1, indicating the importance of CH_4 emission. The ebullitive CH_4 flux

dominated the GHG emission, with a share of 75% of total CH_4 emission and 50% of total GHG emission. From October until February, CO_2 formed the majority of GHG emission, with a share of 80% to 96%. The CH_4 emissions were low during these coldest months (< 0.5 g CO_2 eq m^{-2} d^{-1}), and more than 85% of methane released by the sediment was oxidized (Fig. 3). No significant temporal (LMM: $F_{1,10} = 2.87$; $p = 0.12$) and spatial (LMM: $F_{1,10} = 4.09$; $p = 0.07$) difference in diffusive CO_2 flux was found. Similarly, there was no significant temporal (LMM: $F_{1,10} = 3.01$; $p = 0.11$) nor spatial (LMM: $F_{1,10} = 2.61$; $p = 0.14$) difference in diffusive CH_4 emission, although the emission was mostly higher in the central zone (Supporting Information Fig. S1). For ebullition, we found a significant main effect of location (GLMM: Wald $t = 2.18$; $p = 0.029$), with higher ebullition in the center of the pond. In addition, we found a significant
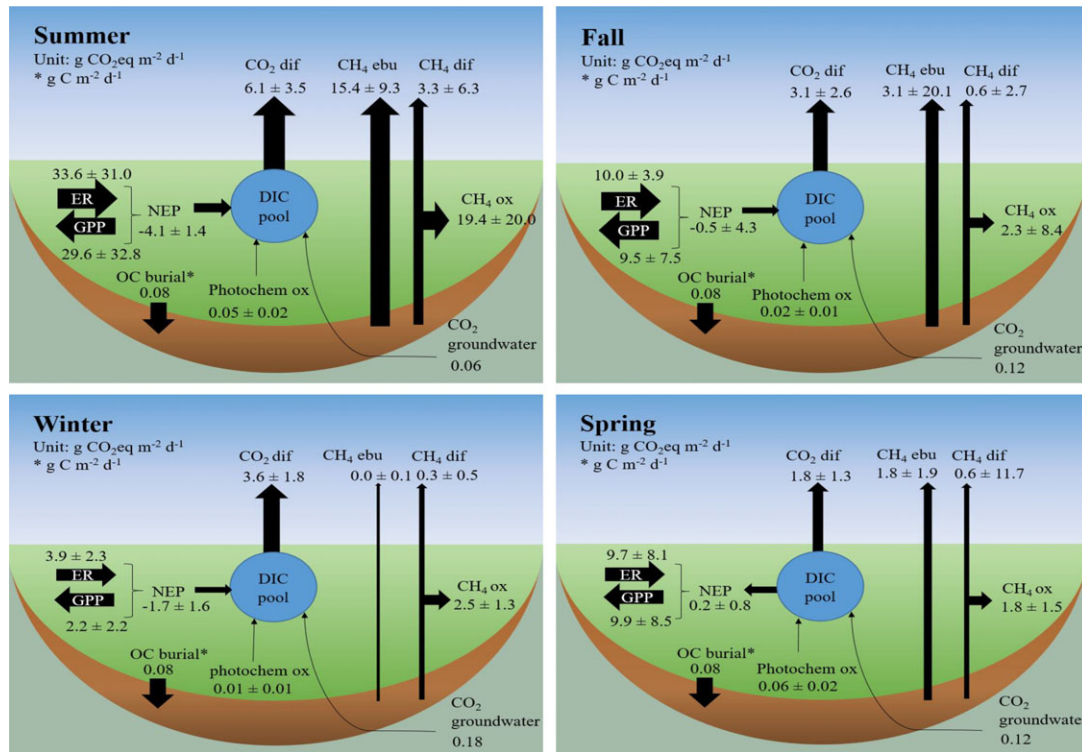
Fig. 3. Seasonal carbon fluxes measured in the pond ± SD. All values are in g CO_2 eq m^{-2} d^{-1}, except for OC burial (g C m^{-2} d^{-1}). A negative NEP indicates ER exceeded GPP, thereby adding to the DIC pool. A positive NEP (GPP > ER) indicates consumption of DIC. Arrows depict the direction of C transport.

interaction (GLMM: Wald t = 2.66; p = 0.008) between time and location: the effect of the center vs. the littoral zone of the pond was higher for nighttime than for daytime CH_4 ebullition rates.

Relative importance of hydrological inputs and within-pond CO_2 production

High GPP rates were found throughout the year (average of 3.30 ± 2.79 g CO_2-C m^{-2} d^{-1}); however, high rates of ER were observed as well (3.66 ± 2.66 g CO_2-C m^{-2} d^{-1}). On average, ER rates exceeded GPP rates, which led to net heterotrophy in the system (average NEP of −0.36 ± 0.69 g CO_2-C m^{-2} d^{-1}). We found net heterotrophy in the system in 8 out of 11 months (NEP of −0.64 ± 0.48 g CO_2-C m^{-2} d^{-1}) and (minor) net autotrophy in the months February, March, and September (with a respective NEP of 0.02, 0.30, and 1.08 g CO_2-C m^{-2} d^{-1}). In months where ER exceeded GPP, the contribution of the NEP to the measured CO_2 emission from the pond was approximately 50% on average. In months with net autotrophy (GPP > ER), the pond still emitted CO_2. When CO_2 inputs from groundwater (yearly average of 0.03 ± 0.01 g C m^{-2} d^{-1}) and CO_2 formed by photochemical mineralization of DOC (yearly average of 0.009 ± 0.007 g C m^{-2} d^{-1}) were added to the NEP in months with net heterotrophy (indicating CO_2 production), the contribution to the measured CO_2 emission was 56%.

Partitioning of ER between organism groups

Empirical relations found to predict organism group-specific respiration (Supporting Information Table S1), based on the relationship between temperature and respiration rates, failed to accurately predict the measured ER of the system (based on the nighttime O_2 decrease at 50 cm depth; Supporting Information Fig. S2). The sum of the modeled respiration of the different organism groups only accounted for roughly half (56%) of the aerobic ER, estimated from the nighttime O_2 curve (Supporting Information Fig. S3). Phytoplankton respiration contributed most to the modeled aerobic ER, with 34.7% on average. After that, the heterotrophic picoplankton and sediment organisms in the lake contributed most to ER with 26.8% and 24.3%, respectively. Fish and methanotrophs contributed the least to ER, with 8.9% and 5.3%, respectively.

Discussion

Our findings demonstrate that the temperate urban pond was a year-round source of GHG, with a particularly large CH_4 emission. The areal GHG emitted by the pond was 3.4 kg CO_2 eq m^{-2} yr^{-1}, which corresponds to 15.5 t of CO_2 equivalents emitted from the pond surface per year. CH_4 ebullition was by far the most important GHG emission pathway (~ 50% of total emission), especially during warm months as we hypothesized (> 15°C, mostly in spring and summer), while

diffusive CH_4 and CO_2 emission contributed with 12% and 38%, respectively. The diffusive CH_4 emission from this small urban pond was three times higher than the average emission reported for small waterbodies within the same size class (on average 0.01 g CH_4 m^{-2} d^{-1}, size class 0.001–0.01 km^2; Holgerson and Raymond 2016). Moreover, the total CH_4 emission (168 mg CH_4 m^{-2} d^{-1}) is moderately high compared to other temperate lakes, irrespective of lake size (Supporting Information Table S3). The OC burial rate corresponded to approximately 6% of the total C emission from the pond (443 g C m^{-2} yr^{-1}), which is rather low, as a recent global analyses indicate that on average lakes and reservoir C burial corresponds to roughly 20% of their emissions (Mendonça et al. 2017). Opposed to our hypothesis, the pond did not shift between a net C source in fall and winter to a net C sink in spring and summer. The pond emitted CO_2 to the atmosphere throughout the entire year, even in months where diel oxygen curves indicated the pond was net autotrophic, suggesting that external CO_2 sources other than within-system aerobic respiration play an important role. Overall, the urban pond acted as a "carbon hub," receiving carbon from different sources, processing, and redirecting the carbon in different ways.

Sediment CH_4 release was strongly related to water temperature and increased exponentially above $15°C$ (Fig. 2), mainly due to increased ebullition. This result corroborates findings in other systems in various climate regions where temperature-induced exponential increases in ebullition were observed (Aben et al. 2017). Nutrients and organic C limitation may constrain sediment CH_4 release and thereby impede its increase with warming (Kelly and Chynoweth 1981; Schwarz et al. 2008; DelSontro et al. 2016). This is, however, unlikely to occur in hypereutrophic urban ponds, where labile OM availability tends to be high throughout the year both due to internal production and external inflow. The high OM availability and anoxic conditions in pond sediments, combined with the shallow water layer, readily explain the high rates of CH_4 ebullition in our pond (Sobek et al. 2012; Martinez-Cruz et al. 2017). As these conditions are common in urban ponds (Waajen et al. 2014), our results imply that CH_4 emission from these systems is high and strongly temperature dependent. The increase of CH_4 oxidation with rising temperature was much weaker than that of sediment CH_4 release, which resulted in a high summer CH_4 emission (Fig. 2) and is in accordance with a previous laboratory study (Sepulveda-Jauregui et al. 2018). In fall and winter, a high proportion (over 85%) of CH_4 was oxidized (Fig. 3) and emissions were low. CH_4 oxidation rates in our pond were comparable with rates found in other eutrophic systems, which were in a range between 0 and 0.32 g C m^{-2} d^{-1} (Bastviken 2009). Only during July—when water temperature was the highest recorded ($25°C$)—we found a rate exceeding the reported range (0.58 g C m^{-2} d^{-1}). Notably, our estimates do not incorporate oxidation at the sediment–water interface, which can be considerable (Bastviken 2009; Martinez-Cruz et al. 2018).

Diffusive CO_2 emission was, after CH_4 ebullition, the most important contributor to the pond's total GHG emission. The internally produced CO_2 (NEP), calculated based on diel O_2 curves, was always lower than the measured CO_2 emission rates (comprising on average ~ 50% of the emission rate). Even during phytoplankton blooms in summer, when GPP exceeded ER, CO_2 was emitted to the atmosphere (6.1 ± 3.5 g CO_2-C m^{-2} d^{-1}). Daytime an nighttime CO_2 emissions were not statistically different. This indicates that the pond's atmospheric CO_2 exchange was not strongly regulated by primary production within the lake, opposed to our hypothesis and to findings of Pacheco et al. (2013). CO_2 input from groundwater and photochemical mineralization of DOC was responsible for approximately 6% of the measured CO_2 emission. The unexplained fraction of the CO_2 emission likely originates from endogenous anaerobic CO_2 production or exogenously produced CO_2 (entering via runoff or local groundwater originating from e.g., leaves from trees, street dirt, or bird droppings). Endogenous anaerobic CO_2 may arise from denitrification, which seems likely as Dutch groundwater often contains a large amount of nitrate (Smolders et al. 2006). Allochthonous C is known to drive CO_2 emission in small and shallow ponds, owing to their high perimeter to volume ratio (Finlay et al. 2010; Holgerson 2015; Wilkinson et al. 2016). Other possible factors that may explain the discrepancy between the measured CO_2 emission and estimated internal CO_2 production include inaccurate estimates of oxygen saturation and gas transfer velocity, as well as a possible underestimation of daytime respiration (Del Giorgio and Williams 2005; Staehr et al. 2010; Brothers et al. 2017). Estimating respiration rates per organism group is a difficult practice as well and comes with several uncertainties and caveats (Del Giorgio and Williams 2005; Martínez-García et al. 2013), which was confirmed by the fact that our modeled ER only accounted for roughly half of the oxygen diel-curve–derived ER.

Seasonal trends in GHG emissions from temperate ponds have generally been disregarded based on the observation that GHG emissions in these systems are often not primarily driven by the seasonally varying within-system metabolism (Jonsson et al. 2003; Holgerson 2015). Although in our pond NEP played a minor role in driving C emission as well, we did find a clear seasonal pattern in GHG emissions (Figs. 1, 3). This seasonal trend is strongly determined by ebullition (Fig. 1; Supporting Information Table S2). We found a lower CO_2 : CH_4 emission ratio with increasing temperature (Supporting Information Table S2), largely due to an increase in CH_4 emission, in accordance with other studies (Yvon-Durocher et al. 2014; DelSontro et al. 2016). Unexpectedly, we did not find clear differences in spatial and temporal (daytime or nighttime) diffusive GHG emission. Both, CH_4 ebullition and diffusion were, however, clearly related to temperature and ebullition was significantly higher in the central zone of the pond. The latter contradicts other studies that suggest the littoral zone plays a more important role in GHG emissions (Natchimuthu et al. 2016). Because of the high spatiotemporal variation in total GHG emission and the high importance of CH_4

ebullition, we recommend future studies to explicitly incorporate ebullition measurements and to take spatial differences into account even in small systems, such as ponds. Furthermore, future monitoring efforts in comparable temperate and eutrophic systems should be concentrated in the months May through September, as in these months the highest fluxes and highest variation occurs. A low number of measurements in fall and winter can be used to estimate cold season emissions.

Extrapolating our findings to all urban ponds in the Netherlands (extrapolated from data by Waajen et al. [2014]), we find a GHG emission of 0.27 Mt CO_2 eq yr^{-1}. This equals the annual emission of approximately 193,000 cars (based on driving 13,200 km yr^{-1}). City planners consider ponds as natural cooling mechanisms to mitigate urban heat stress (Inard et al. 2004; Theeuwes et al. 2013); however, our findings indicate that this is not a GHG neutral option. In addition, hypereutrophic urban ponds are more likely to be affected by raising temperatures, as water temperatures of small and shallow water systems are closely correlated to air temperature, making them sensitive to rapid warming (Toffolon et al. 2014; Wik et al. 2014). Shallow, urban ponds with a high OM input may thus likely exhibit enhanced CH_4 emissions with global warming induced rising of water temperatures (O'Reilly et al. 2015). Considering their already high GHG emission rates, their inclusion in regional GHG emission assessments is important. Climate change will likely feedback on urban ponds GHG emissions and additionally worsen eutrophication and OM loading to the system (Moss et al. 2011). In line with the idea of using local management strategies to mitigate global stressors (Scheffer et al. 2015), management strategies for urban ponds should be aimed at reducing eutrophication and OM loading. In this way, local management may counteract the warming induced increase of GHG emissions as well.

References

Aben, R. C., and others. 2017. Cross continental increase in methane ebullition under climate change. Nat. Commun. **8**: 1682. doi:10.1038/s41467-017-01535-y

Algesten, G., S. Sobek, A. K. Bergström, A. Ågren, L. J. Tranvik, and M. Jansson. 2003. Role of lakes for organic carbon cycling in the boreal zone. Glob. Chang. Biol. **10**: 141–147. doi:10.1046/j.1529-8817.2003.00721.x

Almeida, R. M., and others. 2016. High primary production contrasts with intense carbon emission in a eutrophic tropical reservoir. Front. Microbiol. **7**: 717. doi:10.3389/fmicb.2016.00717

Balmer, M. B., and J. A. Downing. 2011. Carbon dioxide concentrations in eutrophic lakes: Undersaturation implies atmospheric uptake. Inland Waters **1**: 125–132. doi:10.5268/IW-1.2.366

Bastviken, D. 2009. Methane. *In* G. E. Likens [ed.], Encyclopedia of inland waters. Elsevier.

Bastviken, D., J. J. Cole, M. L. Pace, and M. C. Van de Bogert. 2008. Fates of methane from different lake habitats: Connecting whole-lake budgets and CH_4 emissions. J. Geophys. Res. Biogeosci. **113**: G02024. doi:10.1029/2007JG000608

Bastviken, D., L. J. Tranvik, J. A. Downing, P. M. Crill, and A. Enrich-Prast. 2011. Freshwater methane emissions offset the continental carbon sink. Science **331**: 50. doi:10.1126/science.1196808

Bates, D., M. Mächler, B. Bolker, and S. Walker. 2015. Fitting linear mixed-effects models using lme4. J. Stat. Softw. **67**: 1–48. doi:10.18637/jss.v067.i01.

Bolund, P., and S. Hunhammar. 1999. Ecosystem services in urban areas. Ecol. Econ. **29**: 293–301. doi:10.1016/S0921-8009(99)00013-0

Brothers, S., G. Kazanjian, J. Köhler, U. Scharfenberger, and S. Hilt. 2017. Convective mixing and high littoral production established systematic errors in the diel oxygen curves of a shallow, eutrophic lake. Limnol. Oceanogr.: Methods **15**: 429–435. doi:10.1002/lom3.10169

Casper, P., S. C. Maberly, G. H. Hall, and B. J. Finlay. 2000. Fluxes of methane and carbon dioxide from a small productive lake to the atmosphere. Biogeochemistry **49**: 1–19. doi:10.1023/A:1006269900174

Champion, T. 2001. Urbanization, suburbanization, counterurbanization and reurbanization, p. 143–161. *In* R. Paddison [ed.], Handbook of urban studies. London: Sage.

Cole, J. J., N. F. Caraco, G. W. Kling, and T. K. Kratz. 1994. Carbon dioxide supersaturation in the surface waters of lakes. Science **265**: 1568–1570. doi:10.1126/science.265.5178.1568

Cole, J. J., M. L. Pace, S. R. Carpenter, and J. F. Kitchell. 2000. Persistence of net heterotrophy in lakes during nutrient addition and food web manipulations. Limnol. Oceanogr. **45**: 1718–1730. doi:10.4319/lo.2000.45.8.1718

Dean, W. E., and E. Gorham. 1998. Magnitude and significance of carbon burial in lakes, reservoirs, and peatlands. Geology **26**: 535–538. doi:10.1130/0091-7613(1998)026<0535:MASOCB>2.3.CO;2

Del Giorgio, P. A., and P. J. l. B. Williams. 2005. Respiration in aquatic ecosystems. Oxford Univ. Press.

DelSontro, T., L. Boutet, A. St-Pierre, P. A. del Giorgio, and Y. T. Prairie. 2016. Methane ebullition and diffusion from northern ponds and lakes regulated by the interaction between temperature and system productivity. Limnol. Oceanogr. **61**: S62–S77. doi:10.1002/lno.10335

Downing, J. A. 2010. Emerging global role of small lakes and ponds: Little things mean a lot. Limnetica **29**: 9–24.

Downing, J. A., and others. 2006. The global abundance and size distribution of lakes, ponds, and impoundments. Limnol. Oceanogr. **51**: 2388–2397. doi:10.4319/lo.2006.51.5.2388

Finlay, K., P. Leavitt, A. Patoine, A. Patoine, and B. Wissel. 2010. Magnitudes and controls of organic and inorganic carbon flux through a chain of hard-water lakes on the

northern Great Plains. Limnol. Oceanogr. **55**: 1551–1564. doi:10.4319/lo.2010.55.4.1551

Gledhill, D. G., P. James, and D. H. Davies. 2008. Pond density as a determinant of aquatic species richness in an urban landscape. Landsc. Ecol. **23**: 1219–1230. doi:10.1007/s10980-008-9292-x

Grasshoff, K., and H. Johannsen. 1972. A new sensitive and direct method for the automatic determination of ammonia in sea water. ICES J. Mar. Sci. **34**: 516–521. doi:10.1093/icesjms/34.3.516

Hanson, P. C., S. R. Carpenter, J. A. Cardille, M. T. Coe, and L. A. Winslow. 2007. Small lakes dominate a random sample of regional lake characteristics. Freshwater Biol. **52**: 814–822. doi:10.1111/j.1365-2427.2007.01730.x

Holgerson, M. A. 2015. Drivers of carbon dioxide and methane supersaturation in small, temporary ponds. Biogeochemistry **124**: 305–318. doi:10.1007/s10533-015-0099-y

Holgerson, M. A., and P. A. Raymond. 2016. Large contribution to inland water CO_2 and CH_4 emissions from very small ponds. Nat. Geosci. **9**: 222–226. doi:10.1038/NGEO2654

Inard, C., D. Groleau, and M. Musy. 2004. Energy balance study of water ponds and its influence on building energy consumption. Build. Serv. Eng. Res. Technol. **25**: 171–182. doi:10.1191/0143624404bt106oa

Jonsson, A., J. Karlsson, and M. Jansson. 2003. Sources of carbon dioxide supersaturation in clearwater and humic lakes in northern Sweden. Ecosystems **6**: 224–235. doi:10.1007/s10021-002-0200-y

Kamphake, L., S. Hannah, and J. Cohen. 1967. Automated analysis for nitrate by hydrazine reduction. Water Res. **1**: 205–216. doi:10.1016/0043-1354(67)90011-5

Kelly, C. A., and D. P. Chynoweth. 1981. The contributions of temperature and of the input of organic matter in controlling rates of sediment methanogenesis. Limnol. Oceanogr. **26**: 891–897. doi:10.4319/lo.1981.26.5.0891

Kosten, S., F. Roland, D. M. L. Da Motta Marques, E. H. Van Nes, N. M. L. d. S. L. Sternberg, M. Scheffer, and J. J. Cole. 2010. Climate-dependent CO_2 emissions from lakes. Global Biogeochem. Cycles **24**: 24. doi:10.1029/2009GB003618

Martinez-Cruz, K., R. Gonzalez-Valencia, A. Sepulveda-Jauregui, F. Plascencia-Hernandez, Y. Belmonte-Izquierdo, and F. Thalasso. 2017. Methane emission from aquatic ecosystems of Mexico City. Aquat. Sci. **79**: 159–169. doi:10.1007/s00027-016-0487-y

Martinez-Cruz, K., A. Sepulveda-Jauregui, P. Casper, K. W. Anthony, K. A. Smemo, and F. Thalasso. 2018. Ubiquitous and significant anaerobic oxidation of methane in freshwater lake sediments. Water Res. **144**: 332–340. doi:10.1016/j.watres.2018.07.053

Martínez-García, S., E. Fernández, D. A. del Valle, D. M. Karl, and E. Teira. 2013. Experimental assessment of marine bacterial respiration. Aquat. Microb. Ecol. **70**: 189–205. doi:10.3354/ame01644

Mendonça, R., S. Kosten, S. Sobek, J. J. Cole, A. C. Bastos, A. L. Albuquerque, S. J. Cardoso, and F. Roland. 2014. Carbon sequestration in a large hydroelectric reservoir: An integrative seismic approach. Ecosystems **17**: 430–441. doi:10.1007/s10021-013-9735-3

Mendonça, R., R. A. Müller, D. Clow, C. Verpoorter, P. Raymond, L. J. Tranvik, and S. Sobek. 2017. Organic carbon burial in global lakes and reservoirs. Nat. Commun. **8**: 1694. doi:10.1038/s41467-017-01789-6

Moss, B., and others. 2011. Allied attack: Climate change and eutrophication. Inland Waters **1**: 101–105. doi:10.5268/IW-1.2.359

Myhre, G., and others. 2013. Anthropogenic and natural radiative forcing, p. 659–740. *In* T. F. Stocker et al. [eds.], Climate change 2013: The physical science basis. Contribution of Working Group I to the fifth assessment report of the intergovernmental panel on climate change. Cambridge Univ. press.

Natchimuthu, S., I. Sundgren, M. Gålfalk, L. Klemedtsson, P. Crill, Å. Danielsson, and D. Bastviken. 2016. Spatiotemporal variability of lake CH_4 fluxes and its influence on annual whole lake emission estimates. Limnol. Oceanogr. **61**: S13–S26. doi:10.1002/lno.10222

Novotny, V. 1999. Integrating diffuse-nonpoint pollution control and water body restoration into watershed management. J. Am. Water Resour. Assoc. **35**: 717–727. doi:10.1111/j.1752-1688.1999.tb04169.x

O'Reilly, C. M., and others. 2015. Rapid and highly variable warming of lake surface waters around the globe. Geophys. Res. Lett. **42**: 10,773–710,781. doi:10.1002/2015GL066235

Pacheco, F. S., F. Roland, and J. A. Downing. 2013. Eutrophication reverses whole-lake carbon budgets. Inland Waters **4**: 41–48. doi:10.5268/IW-4.1.614

Raymond, P. A., and others. 2013. Global carbon dioxide emissions from inland waters. Nature **503**: 355–387. doi:10.1038/nature12760

Roland, F., L. O. Vidal, F. S. Pacheco, N. O. Barros, A. Assireu, J. P. H. B. Ometto, A. C. P. Cimbleris, and J. J. Cole. 2010. Variability of carbon dioxide flux from tropical (Cerrado) hydroelectric reservoirs. Aquat. Sci. **72**: 283–293. doi:10.1007/s00027-010-0140-0

Sand-Jensen, K., and P. A. Staehr. 2009. Net heterotrophy in small Danish lakes: A widespread feature over gradients in trophic status and land cover. Ecosystems **12**: 336–348. doi:10.1007/s10021-008-9226-0

Scheffer, M., and others. 2015. Creating a safe operating space for iconic ecosystems. Science **347**: 1317–1319. doi:10.1126/science.aaa3769

Scherer, N. M., H. L. Gibbons, K. B. Stoops, and M. Muller. 1995. Phosphorus loading of an urban lake by bird droppings. Lake Reservoir Manage. **11**: 317–327. doi:10.1080/07438149509354213

Schwarz, J. I., W. Eckert, and R. Conrad. 2008. Response of the methanogenic microbial community of a profundal Lake

sediment (Lake Kinneret, Israel) to algal deposition. Limnol. Oceanogr. **53**: 113–121. doi:10.4319/lo.2008.53.1.0113

Sepulveda-Jauregui, A., J. Hoyos-Santillan, K. Martinez-Cruz, K. M. Walter Anthony, P. Casper, Y. Belmonte-Izquierdo, and F. Thalasso. 2018. Eutrophication exacerbates the impact of climate warming on lake methane emission. Sci. Total Environ. **636**: 411–419. doi:10.1016/j.scitotenv.2018.04.283

Smith, V. H. 1979. Nutrient dependence of primary productivity in lakes. Limnol. Oceanogr. **24**: 1051–1064. doi:10.4319/lo.1979.24.6.1051

Smolders, A., L. Lamers, E. Lucassen, G. Van der Velde, and J. Roelofs. 2006. Internal eutrophication: How it works and what to do about it—a review. Chem. Ecol. **22**: 93–111. doi:10.1080/02757540600579730

Sobek, S., T. DelSontro, N. Wongfun, and B. Wehrli. 2012. Extreme organic carbon burial fuels intense methane bubbling in a temperate reservoir. Geophys. Res. Lett. **39**: L01401. doi:10.1029/2011GL050144

Staehr, P. A., D. Bade, M. C. Van de Bogert, G. R. Koch, C. Williamson, P. Hanson, J. J. Cole, and T. Kratz. 2010. Lake metabolism and the diel oxygen technique: State of the science. Limnol. Oceanogr.: Methods **8**: 628–644. doi:10.4319/lom.2010.8.628

Theeuwes, N., A. Solcerová, and G. Steeneveld. 2013. Modeling the influence of open water surfaces on the summertime temperature and thermal comfort in the city. J. Geophys. Res.: Atmos. **118**: 8881–8896. doi:10.1002/jgrd.50704

Toffolon, M., S. Piccolroaz, B. Majone, A.-. M. Soja, F. Peeters, M. Schmid, and A. Wüest. 2014. Prediction of surface temperature in lakes with different morphology using air temperature. Limnol. Oceanography **59**: 2185–2202. doi:10.4319/lo.2014.59.6.2185

Tranvik, L. J., and others. 2009. Lakes and reservoirs as regulators of carbon cycling and climate. Limnol. Oceanog. **54**: 2298–2314. doi:10.4319/lo.2009.54.6_part_2.2298

Trolle, D., P. A. Staehr, T. A. Davidson, R. Bjerring, T. L. Lauridsen, M. Søndergaard, and E. Jeppesen. 2012. Seasonal dynamics of CO_2 flux across the surface of shallow temperate lakes. Ecosystems **15**: 336–347. doi:10.1007/s10021-011-9513-z

Vähätalo, A. V., M. Salkinoja-Salonen, P. Taalas, and K. Salonen. 2000. Spectrum of the quantum yield for photochemical mineralization of dissolved organic carbon in a humic lake. Limnol. Oceanogr. **45**: 664–676. doi:10.4319/lo.2000.45.3.0664

Verpoorter, C., T. Kutser, D. A. Seekell, and L. J. Tranvik. 2014. A global inventory of lakes based on high-resolution satellite imagery. Geophys. Res. Lett. **41**: 6396–6402. doi:10.1002/2014GL060641

Waajen, G. W., E. J. Faassen, and M. Lürling. 2014. Eutrophic urban ponds suffer from cyanobacterial blooms: Dutch examples. Environ. Sci. Pollut. Res. **21**: 9983–9994. doi:10.1007/s11356-014-2948-y

Waschbusch, R. J., W. R. Selbig, and R. T. Bannerman. 1999. Sources of phosphorus in stormwater and street dirt from two urban residential basins in Madison, Wisconsin, 1994-95, p. 51. Water-Resources Investigations Report.

West, W. E., J. J. Coloso, and S. E. Jones. 2012. Effects of algal and terrestrial carbon on methane production rates and methanogen community structure in a temperate lake sediment. Freshwater Biol. **57**: 949–955. doi:10.1111/j.1365-2427.2012.02755.x

West, W. E., K. P. Creamer, and S. E. Jones. 2016. Productivity and depth regulate lake contributions to atmospheric methane. Limnol. Oceanogr. **61**: S51–S61. doi:10.1002/lno.10247

Weyhenmeyer, G. A., S. Kosten, M. B. Wallin, L. J. Tranvik, E. Jeppesen, and F. Roland. 2015. Significant fraction of CO_2 emissions from boreal lakes derived from hydrologic inorganic carbon inputs. Nat. Geosci. **8**: 933–936. doi:10.1038/ngeo2582

Wik, M., B. F. Thornton, D. Bastviken, S. MacIntyre, R. K. Varner, and P. M. Crill. 2014. Energy input is primary controller of methane bubbling in subarctic lakes. Geophys. Res. Lett. **41**: 555–560. doi:10.1002/2013GL058510

Wik, M., R. K. Varner, K. W. Anthony, S. MacIntyre, and D. Bastviken. 2016. Climate-sensitive northern lakes and ponds are critical components of methane release. Nat. Geosci. **9**: 99–105. doi:10.1038/NGEO2578

Wilkinson, G. M., C. D. Buelo, J. J. Cole, and M. L. Pace. 2016. Exogenously produced CO_2 doubles the CO_2 efflux from three north temperate lakes. Geophys. Res. Lett. **43**: 1996–2003. doi:10.1002/2016GL067732

Wong, T., P. F. Breen, and S. D. Lloyd. 2000. Water sensitive road design: Design options for improving stormwater quality of road runoff. CooperativeCenter for Catchment Hydrology.

Yvon-Durocher, G., A. P. Allen, D. Bastviken, R. Conrad, C. Gudasz, A. St-Pierre, N. Thanh-Duc, and P. A. del Giorgio. 2014. Methane fluxes show consistent temperature dependence across microbial to ecosystem scales. Nature **507**: 488–491. doi:10.1038/nature13164

Conflict of Interest

None declared

Author Contribution Statement

V.H., M.L., and S.K. initiated the overarching project. N.B, R.M. and S.K. initiated the study present in the paper. N.B., R.M., T.J.H.M. v.B and I.H.J.A. conducted the fieldwork. T.J.H.M.v.B and N.B. analysed the data. I.H.J.A. and N.B. conducted the sediment incubation. R.A. contributed to the statistical analyses. T.J.H.M.v.B. did the majority of the manuscript writing. T.J.H.M.v.B., N.B., R.M., R.A., I.H. J.A., V.H., L.P.M.L., M.L., F.R. and S.K. contributed to revisions of the manuscript.